Optics Communications 389 (2017) 74–78

Contents lists available at ScienceDirect

Optics Communications

journal homepage: www.elsevier.com/locate/optcom

Membrane-less variable focus liquid lens with manual actuation

Roshan Patra[a,1], Shivam Agarwal[a,1], Sasidhar Kondaraju[b], Supreet Singh Bahga[a,*]

[a] Indian Institute of Technology Delhi, Hauz Khas, New Delhi 110016, India
[b] Indian Institute of Technology Bhubaneswar, Bhubaneswar, Orrisa 751013, India

ARTICLE INFO

Keywords:
Liquid lens
Adaptive optics
Mechanical-wetting lens
Interface pinning

ABSTRACT

We present a tunable, membrane-less, mechanical-wetting liquid lens that can be actuated manually using a linear actuator such as screw or piston. The operation of the liquid lens is based on deforming the interface separating two immiscible liquids with different refractive indices, while pinning the three-phase contact line at the sharp edge of lens aperture. Our lens design improves upon the existing designs of mechanical-wetting lenses by eliminating the use of complex actuation mechanisms, without compromising on the optical performance. We demonstrate the operation of the liquid lens by tuning its power back and forth from negative to positive by simple rotation of a screw. We also present an analytical description of the focal length of the lens and validate it with detailed experimental measurements. Our experiments show that the focal length of the liquid lens can be tuned repeatably without any adverse effects of hysteresis and gravity.

1. Introduction

Variable focus lenses have seen a significant interest over past decade due to their potential of replacing bulky lens assemblies consisting of fixed focal length lenses [1–3]. Using liquids as deformable, refracting media offers a convenient way of fabricating variable focus lenses [1,2]. Unlike conventional optical systems, which require varying distance between fixed-focal length lenses, liquid lenses give same functionality by varying the curvature and thus eliminating relative movement between the lenses. Therefore, the compactness of liquid lenses makes them suitable for miniaturized optical systems, such as mobile phones and surveillance cameras. Liquid lenses have found a variety of applications, such as in digital cameras [4,5], microscopy [6–8], and laser materials processing [9]. Numerous approaches for varying the liquid interface curvature in liquid lenses have been demonstrated. The approaches can be broadly classified into: (i) those based on a transparent elastic membrane to hold the liquid [10–13], and (ii) those based on using the interface between two immiscible liquids as the deformable surface [4,14].

In membrane-type liquid lenses, the liquid is kept in a transparent chamber having an optically transparent elastic membrane as the chamber boundary [10–13]. The curvature of the membrane is changed either by pumping the liquid in or out of the chamber or by increasing the pressure inside the chamber which deforms the elastic membrane. The lens profile is determined solely by the mechanical properties of the elastic membrane. Therefore, by controlling the mechanical properties of the membrane, aspherical lenses can be obtained [15]. However, mechanical fatigue of the elastic membrane, variation in its elastic properties over time, and physical imperfections limit the lens performance. In addition, membrane-type lenses are sensitive to their orientation as gravity effects can cause the lens to acquire asymmetric shape, thereby deteriorating the optical performance.

In contrast to membrane-type liquid lenses, membrane-less liquid lenses employ the interface separating two immiscible, optically transparent liquids with different indices of refraction [16–21] as the deformable surface. The liquid-liquid interface is very smooth compared with an elastic membrane and is devoid of mechanical fatigue. The liquid-liquid interface however intrinsically acquires a spherical shape that can lead to spherical aberration. As opposed to membrane-type liquid lenses, the adverse effects of gravity can be eliminated in membrane-less liquid lenses by choosing two liquids with equal densities [22]. The most common example of a membrane-less liquid lens is the electrowetting lens, pioneered by Berge et al. [16]. This lens leverages electrowetting phenomenon to vary contact angle of a conducting liquid on a non-conductive surface by applying a potential difference between the liquid and the surface. The electrowetting lens typically requires a relatively high voltage of order 100 V for actuation and suffers from electrolysis, Joule heating, bubble formation due to applied electric field, and contact angle hysteresis [23].

These drawbacks of electrowetting lenses can be eliminated in membrane-less liquid lenses [17–21] wherein the three-phase contact

* Corresponding author.
E-mail address: bahga@mech.iitd.ac.in (S.S. Bahga).
[1] Equal contribution.

http://dx.doi.org/10.1016/j.optcom.2016.12.021
Received 5 September 2016; Received in revised form 5 December 2016; Accepted 7 December 2016

line between two liquids and the solid surface is pinned to the surface [24]. In these so-called “mechanical-wetting” lenses, a sharp change in geometry or wettability of the surface is used to pin the contact line. The curvature of the liquid-liquid interface can be deformed by varying the fluid volume or pressure across the interface. Unlike in electrowetting lens, the pinning of contact line in mechanical-wetting lens ensures that the liquid-liquid interface remains self-centered on the optical axis. Moreover, unlike electrowetting lenses, mechanical-wetting lenses do not suffer from focal length hysteresis as the latter's operation does not depend on the motion of contact line [20].

The existing designs and actuation mechanisms of membrane-less, mechanical-wetting lenses involve either deformable lens walls [17], piezoelectric transducers [18], ferrofluids actuated by a magnetic field [19,20], or thermoresponsive hydrogels [21] to apply pressure on the liquids. Actuation of mechanical-wetting lenses using piezoelectric transducers [18] and magnetic field [19] have been shown to yield fast tuning capability with response time of 2 ms. However, the existing actuation methods and the lens designs are relatively complex and expensive in construction, which preclude their integration with low-cost optical systems such as mobile phones and webcams. We here present a simple design of mechanical-wetting liquid lens which can be actuated manually using a linear actuator such as screw or piston. Our design of the variable focus liquid lens retains the advantages of other designs of mechanical-wetting lenses, such as high resolution, no gravity effect, and wide dynamic range, while simplifying the actuation mechanism and reducing the cost of fabrication.

2. Design

In Fig. 1, we present a schematic of our membrane-less liquid lens. The assembly of the liquid lens consists of a top chamber and a bottom chamber, separated by an aperture. The liquid lens is provided with optically clear top and bottom windows which are perpendicular to the optical axis. The top and bottom chambers contain different liquids which are immiscible and have different refraction indices. In contrast

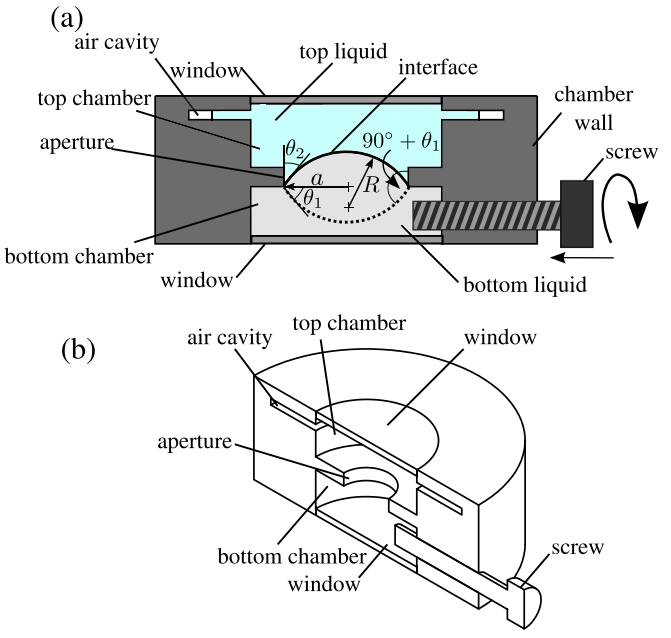

Fig. 1. Schematic showing the design of the membrane-less, mechanical-wetting liquid lens. (a) Sectional side-view of the lens assembly. The lens compartment contains two immiscible fluids with distinct refractive indices. The interface separating the immiscible fluids is pinned at the sharp edge of the aperture. The motion of screw changes the pressure of the bottom liquid which deforms the interface, and thereby varying the focal length. The air cavity in the top chamber compensates for the change in volume of top chamber due to the deformation of interface. (b) Sectional three-dimensional view of the liquid lens assembly.

to the electrowetting lens, there is no requirement for one liquid to be conducting and other to be insulating. The volumes of these two liquids are chosen such that the interface between these two liquids gets pinned to the sharp edge of the aperture as shown in Fig. 1(a). To vary the focal length of the liquid lens, we provide a screw in the bottom chamber which can be manually turned in or out of the chamber. When the screw is turned in or out of the bottom chamber, the pressure of the liquid at the bottom changes which in turn changes the curvature of interface pinned at the aperture. Therefore, the focal length of the lens can be varied by turning the screw in or out of the bottom chamber. To compensate for the change in volume of the top chamber due to the deformation of liquid-liquid interface, we provide a narrow air cavity in which the air (or gas) can compress or expand during the actuation of lens. We note that instead of a screw, other linear actuators such as a piston can also be used in the current lens design. The focal length of liquid lens shown in Fig. 1 can therefore be tuned manually and does not require electrical power for actuation.

To prevent the deformation of liquid-liquid interface due to gravity and make the operation of lens robust for different orientations, the aperture size should be chosen smaller than the capillary length associated with the two fluids, defined as $\sqrt{\gamma/(\Delta\rho g)}$ [24]. Here, γ denotes the interfacial tension, $\Delta\rho$ the difference in densities of two fluids, and g the acceleration due to gravity. This constraint on aperture size can be satisfied by choosing liquids with substantially equal densities. Unlike in membrane-type liquid lenses, the aperture in our membrane-less liquid lens design can be made arbitrarily large if the top and bottom liquids are chosen with identical densities. Similarly, the interface between air (or gas) and the top liquid remains stable for different orientations provided the thickness of air cavity is smaller than the capillary length of top fluid. We note that, the narrow circular air cavity is a key design feature of our liquid lens. Due to the relatively large circumference of interface between air and the top liquid, the motion of air-liquid interface in a narrow cavity is sufficient to compensate for the large change in volume due to the motion of screw.

The liquid lens shown in Fig. 1 can operate both as positive (converging) or negative (diverging) lens depending upon the curvature of the liquid-liquid interface and the relative magnitude of the refractive index of the two liquids. If both the chamber walls have a contact angle of θ_1 with the liquid in top chamber, the contact angle between the top liquid and the vertical aperture surface can be varied from θ_1 to $\theta_1 + 90°$. Therefore, the interfacial shape in the liquid lens shown in Fig. 1 can be varied from concave to convex. Further, to enhance the focal length range of the lens, the inner surfaces of the bottom and top chambers (considering aperture as a part of top chamber) can be treated to have different wettability. If the contact angle of liquid in top chamber is θ_1 and θ_2 with the bottom and top chambers respectively, the contact angle between the top liquid and the aperture surface can be varied from θ_2 to $\theta_1 + 90°$ as shown in Fig. 1; this yields wider variation in the focal length. For example, if the liquid in top chamber makes a contact angle of 70° with bottom chamber and 10° with top chamber, the contact angle at the aperture can be varied from 10° to 160°.

To obtain a relationship between the screw position and the focal length of the lens, we consider a general case wherein the interface curvature can be either convex or concave in the upward direction. Denoting the number of turns given to the screw relative to the position where the interface is initially flat by N, the volume swept by the screw is given by $\Delta V = N\pi r_0^2 l_0$, where r_0 and l_0 denote the radius and the pitch of screw, respectively. Assuming that the lens liquids are incompressible and the liquid-liquid interface is spherical, the volume swept by the screw is equal to the volume of the spherical cap of the interface. That is,

$$\frac{\pi}{6}(-R \pm \sqrt{R^2 - a^2})(3a^2 + (-R \pm \sqrt{R^2 - a^2})^2) = N\pi r_0^2 l_0. \quad (1)$$

where a denotes the radius of aperture and the left hand side of the

equation is the volume of the spherical cap of the interface. In Eq. (1), the radius of curvature R is taken to be positive (negative) when the interface is concave (convex) upwards. Whereas, the number of turns of screw N is taken positive (negative) if the screw moves into (out of) the lens chamber, relative to the position where the liquid-liquid interface is flat. The + and - signs on the left hand side of Eq. (1) correspond to concave and convex interface, respectively.

The focal length of the lens, assuming it to be thin, is given by

$$f = \frac{R}{n_t - n_b}, \tag{2}$$

where n_t and n_b denote the refractive indices of top and bottom fluids, respectively. As shown experimentally in Section 3, the focal length of our lens is significantly larger than the thickness of the lens. Therefore, the assumption of thin lens holds well for our liquid lens. Because the radius of curvature R scales with the aperture radius, for typical values of aperture radius of 2 mm and refractive index difference of $n_t - n_b = 0.1$, Eq. (2) predicts that the tuning range of the lens can be as large as ± 50 diopters.

3. Experiments and results

In the current work, we fabricated the liquid lens shown schematically in Fig. 1 out of acrylic. Acrylic sheets were laser cut to form different layers of the lens assembly, including the top and bottom chambers, and the aperture. The top and bottom chambers were of 15 mm radius and 4 mm thickness. The aperture was 2 mm thick and had a radius of 3 mm. A 2.5 mm hole was drilled laterally into the bottom chamber and an M3 screw (pitch 0.5 mm) was inserted. To prevent leakage of fluid, the screw was wrapped with a teflon sealing tape. The top and bottom windows were cut out of glass. The narrow air cavity was made by inserting a layer of paraffin film to form a spacer between the top chamber and the top wall. We estimated that the thickness of air cavity was about 100 μm. All the layers, except the top layer, were then bonded with to form the lens compartment.

Next, the bottom and the top chambers were filled with deionized water (refractive index n=1.33, density ρ=997 kg m^{-3} at 25 °C) and 1-bromododecane (n=1.46, density ρ=1038 kg m^{-3} at 25 °C), respectively, while ensuring that the interface between the two fluids was pinned at the edge of aperture. Finally, the lens compartment was mechanically clamped with the top window. The paraffin film used as spacer for air cavity between the lens compartment and the top window also acts as a gasket. For water and 1-bromododecane combination, the interfacial tension is 52.6 mN m^{-1} [25] and the corresponding capillary length is 11.4 mm. Since the aperture size of 3 mm radius is significantly smaller than the capillary length, gravity has minimal effect on the shape of liquid-liquid interface. We note that, the densities of both liquids can be made exactly equal by dissolving salt in deionized water.

To evaluate the performance of our variable focus liquid lens, we held a paper with “IIT” printed on it close to the lens and imaged it in white light. Fig. 2 shows the images taken through the lens in vertical orientation, with the plane of aperture parallel to the direction of gravity. Initially, the screw is turned into a position where the water-oil interface is flat. Fig. 2(a) shows the image at this neutral state wherein the size of the picture is same as that without the lens. When the screw is turned into the lens cavity, the water-oil interface attains a convex shape (with respect to bottom chamber). Since the refractive index of oil in the current case is higher than water, turning in the screw results in a diverging lens, as shown in Fig. 2(b). Whereas, turning the screw out of the neutral position results in a converging lens accompanied with a magnified image shown in Fig. 2(c). The results shown in Fig. 2 indicate robust performance of our liquid lens in vertical position where the deformation of liquid-liquid interface due to gravity is maximum. This is because, the densities of two liquids are similar and the aperture radius (3 mm) is smaller than the capillary length of about 11.4 mm. We attribute small aberrations seen in Fig. 2 near the aperture circumference to distortion of the pinned contact line that occurs due to the defects in machining of aperture. The distortion of liquid-liquid interface due to distortion of pinned contact line diminishes with distance from the contact line [22]. Moreover, these defects can be rectified by precise fabrication of the aperture.

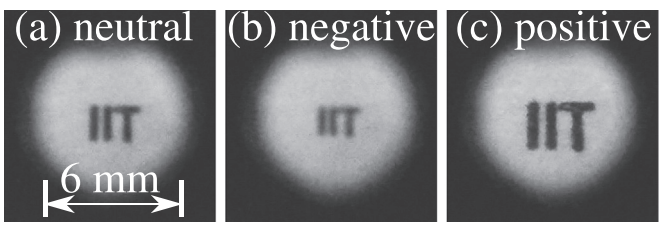

Fig. 2. Images taken through the lens for different positions of the screw. (a) Initially, the screw was turned to the position where the liquid-liquid interface was flat, that is, in the neutral state. The lens attains negative power (b) and positive power (c) when the screw is turned in and out, respectively. For these experiments, the lens was kept vertically such that the plane of aperture is parallel to the direction of gravity.

In our lens design, the top liquid (1-bromododecane) has higher refractive index than the bottom liquid (water). Consequently, the lens works as a converging (diverging) lens when the liquid-liquid interface is concave (convex) upwards. We characterized the performance of our liquid lens by measuring the focal length for varying turns of the screw. Briefly, we passed a beam of parallel light through the lens assembly. When the liquid lens behaved as a diverging lens, we imaged the diverging beam on the other side of the lens at two locations and used the measured diameters of the beams to trigonometrically estimate the focal length. Whereas, when the liquid lens behaved as a converging lens, we obtained the focal point by noting the smallest focused point. We repeated the experiment five times for different number of turns of the screw to obtain the mean back focal distance (BFD) and the standard deviation of mean BFD (using Student's t-distribution).

Fig. 3 shows the variation of focal length with the number of turns of the screw, N. As expected, in both converging and diverging mode, the focal length decreases with the number of turns of screw. As shown in Fig. 3, the focal length is most sensitive to the rotation of screw close to the neutral position. Moreover, the focal length approaches its minimum possible value in approximately one complete turn of the

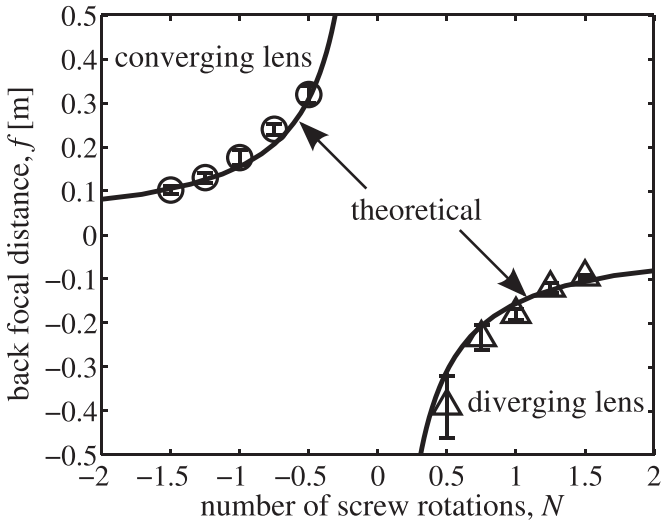

Fig. 3. Measured and theoretically predicted back focal distance (BFD) of liquid lens for varying screw rotations N. The data points show experimental measurements and the solid line shows prediction using Eqs. (1) and (2). Initially, the screw is positioned such that the liquid-liquid interface is flat. The liquid has positive and negative power when the screw is rotated out of or into the lens chamber, respectively. The focal distance is sensitive to the rotation of screw near the neutral position (N = 0), which leads to higher uncertainty in measured BFD near the neutral position.

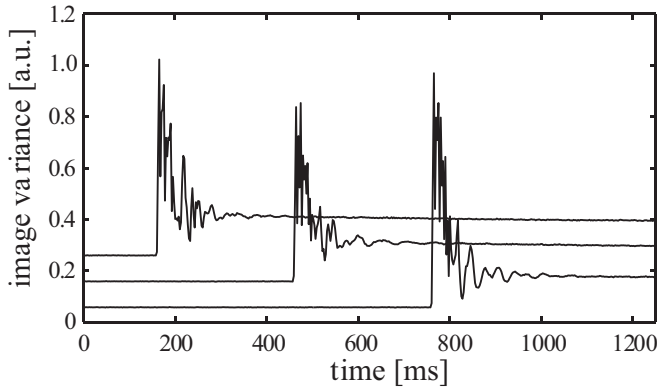

Fig. 4. Transient response of the liquid lens in three repeated experimental runs. The image variance shows oscillations upon sudden actuation. These oscillations diminish completely after 250 ms. The time response of the liquid lens is similar for all the experimental runs.

screw, which suggests that focal length of our lens can be tuned by minimal manual effort. The low uncertainty in focal length measurements presented in Fig. 3 show that the focal length of our lens can be tuned without any hysteresis effect. In Fig. 3, we also show the comparison of experimentally measured focal length with theoretical predicted focal length using Eqs. (1) and (2). The predicted focal length agrees well with the experimental data. Therefore, Eqs. (1) and (2) can be used for choosing design parameters, such as aperture size, pitch and diameter of the screw, and volume of lens chambers to obtain the required lens performance.

In general, the refractive index of lens liquids and hence the focal length depend on the wavelength of light. This leads to dispersion and associated chromatic aberration. To estimate the chromatic aberration of our lens, using Eq. (2), we calculate the difference in focal length corresponding to Fraunhofer F and C lines (wavelength $\lambda_F = 486.1$ nm and $\lambda_C = 656.3$ nm) relative to the focal length at Fraunhofer D line ($\lambda_D = 587.6$ nm). Based on the data of refractive indices of water and 1-bromododecane for specific Fraunhofer wavelengths provided by Liebetraut et al. [26], the relative longitudinal chromatic aberration, given by $(f(\lambda_C) - f(\lambda_F))/f(\lambda_D)$, for our lens is 2.6% for any number of rotations of the screw. We note that, a proper choice of liquids can achromatize the membrane-less liquid lens as the lens system shown in Fig. 1 resembles a cemented doublet. As described by Kuiper et al. [5], achromatization can be achieved if the refractive indices of top and bottom liquids (n_t and n_b) are related to the corresponding Abbe numbers (A_t and A_b) by $A_t/A_b = (n_t(\lambda_D) - 1)/(n_b(\lambda_D) - 1)$.

Finally, we evaluated the response time of our membrane-less liquid lens. Here, we note that the typical time for manual actuation is of order 1 s. Therefore, our lens design is suitable for applications wherein the primary goal is to integrate a compact, low-cost variable focus lens with electronic equipment, rather than rapid tuning of focal length. To check whether the tuning speed of the liquid lens is limited by manual actuation or the dynamics of liquid-liquid interface, we performed experiments similar to those shown in Fig. 2. However, in this case the lens was kept horizontal and the screw was turned quickly with a spring-loaded mechanism, whose actuation time was measured to be about 50 ms using a high speed camera (Andor Zyla 5.5) at 400 fps. When the screw is rotated rapidly, it leads to a rapid change in focal length and magnification of the lens. A series of images were recorded at the rate of 400 fps to capture the transient change in magnification of the lens. In Fig. 4, we show the time dependence of image variance with respect to the initial image at time t_0, defined as $(\sum_x \sum_y (I(x, y; t) - I(x, y; t_0))^2)^{1/2}$, where $I(x, y; t)$ denotes the intensity of the pixel at (x, y) at time t. For three experimental runs shown in Fig. 4, we observe that sudden actuation of the lens leads to a new steady state via transients that last for over 250 ms. In particular, the transient response of liquid lens to the step-input, shown in Fig. 4, exhibits oscillations that are indicative of an under-damped system [4]. The response time of the lens can be further reduced by reducing the aperture radius a and selecting lens liquids with higher kinematic viscosities ν [4]. This reduces the viscous diffusion time a^2/ν and for appropriate choice of aperture size and lens liquids, the liquid-liquid interface can be made critically damped. For example, Oku and Ishikawa [18] demonstrated a mechanical-wetting lens with response time of 2 ms using smaller aperture of 1.5 mm radius and polydimethylsiloxane (PDMS) with high kinematic viscosity of 5000 cSt as the top liquid. Despite the possibility of further reduction in response time, for all practical purposes, even with a response time of 250 ms the tuning speed of our lens is limited by slow manual actuation.

4. Conclusion

In summary, we have presented a simple design of a membrane-less, mechanical-wetting liquid lens that can be actuated manually using a linear actuator such as a screw. Our lens design retains all the advantages of mechanical-wetting lenses, while simplifying the actuation mechanism and the cost of fabrication. We have demonstrated robust operation of our liquid lens with both positive and negative power in vertical orientation, where the adverse effects of gravity on liquid-liquid interface are expected to be maximum. Moreover, we have characterized the focal length of the lens for varying rotations of the screw. Our experiments show that the focal length can be tuned repeatably without any hysteresis. We have presented an analytical description of the focal length of liquid lens, and validated it with experimental data. In the current work, we have demonstrated manual actuation of the liquid lens. However, the lens design allows integration of an electrically controlled actuation, such as a servo motor, for fast and precise control of the focal length. We believe that simple, low-cost, robust, and easy-to-operate design of our liquid lens makes it well-suited for miniaturized optical systems in consumer electronics.

Acknowledgements

This work was supported by the Design Innovation Translational Seed Grant of Design Innovation Centre, Indian Institute of Technology Delhi.

References

[1] C.-P. Chiu, T.-J. Chiang, J.-K. Chen, F.-C. Chang, F.-H. Ko, C.-W. Chu, S.-W. Kuo, S.-K. Fan, Liquid lenses and driving mechanisms:a review, J. Adhes. Sci. Technol. 26 (12–17) (2012) 1773–1788.
[2] Y. Fainman, L. Lee, D. Psaltis, C. Yang, Optofluidics: Fundamentals, Devices, and Applications, McGraw-Hill, Inc., 2009.
[3] P. Liebetraut, S. Petsch, J. Liebeskind, H. Zappe, Elastomeric lenses with tunable astigmatism, Light Sci. Appl. 2 (2013) e98.
[4] S. Kuiper, B. Hendriks, Variable-focus liquid lens for miniature cameras, Appl. Phys. Lett. 85 (7) (2004) 1128–1130.
[5] S. Kuiper, B. Hendriks, J. Suijver, S. Deladi, I. Helwegen, Zoom camera based on liquid lenses, Proceedings SPIE 6466 (2007) 64660F–64660F–7.
[6] N. Koukourakis, M. Finkeldey, M. Stürmer, C. Leithold, N.C. Gerhardt, M.R. Hofmann, U. Wallrabe, J.W. Czarske, A. Fischer, Axial scanning in confocal microscopy employing adaptive lenses (cal), Opt. Express 22 (5) (2014) 6025–6039.
[7] F.O. Fahrbach, F.F. Voigt, B. Schmid, F. Helmchen, J. Huisken, Rapid 3d light-sheet microscopy with a tunable lens, Opt. Express 21 (18) (2013) 21010–21026.
[8] K. Philipp, A. Smolarski, N. Koukourakis, A. Fischer, M. Stürmer, U. Wallrabe, J.W. Czarske, Volumetric hilo microscopy employing an electrically tunable lens, Opt. Express 24 (13) (2016) 15029–15041.
[9] M. Duocastella, C. Arnold, Enhanced depth of field laser processing using an ultra-high-speed axial scanner, Appl. Phys. Lett. 102 (6) (2013) 061113.
[10] H. Ren, S.-T. Wu, Variable-focus liquid lens, Opt. Express 15 (10) (2007) 5931–5936.
[11] H. Ren, S.-T. Wu, Variable-focus liquid lens by changing aperture, Appl. Phys. Lett. 86 (21) (2005) 211107.
[12] R. Kuwano, T. Tokunaga, Y. Otani, N. Umeda, Liquid pressure varifocus lens, Opt. Rev. 12 (5) (2005) 405–408.
[13] P.-H. Cu-Nguyen, A. Grewe, M. Hillenbrand, S. Sinzinger, A. Seifert, H. Zappe, Tunable hyperchromatic lens system for confocal hyperspectral sensing, Opt. Express 21 (23) (2013) 27611–27621.

[14] L. Ren, S. Park, H. Ren, I.-S. Yoo, Adaptive liquid lens by changing aperture, J. Microelectromech S 21 (4) (2012) 953–958.
[15] S.H. Cho, F.S. Tsai, W. Qiao, N.-H. Kim, Y.-H. Lo, Fabrication of aspherical polymer lenses using a tunable liquid-filled mold, Opt. Lett. 34 (5) (2009) 605–607.
[16] B. Berge, J. Peseux, Variable focal lens controlled by an external voltage:an application of electrowetting, Eur. Phys. J. E. 3 (2) (2000) 159–163.
[17] S. Xu, Y. Liu, H. Ren, S.-T. Wu, A novel adaptive mechanical-wetting lens for visible and near infrared imaging, Opt. Express 18 (12) (2010) 12430–12435.
[18] H. Oku, M. Ishikawa, High-speed liquid lens with 2 ms response and 80.3 nm root-mean-square wavefront error, Appl. Phys. Lett. 94 (22) (2009) 221108.
[19] H.-C. Cheng, S. Xu, Y. Liu, S. Levi, S.-T. Wu, Adaptive mechanical-wetting lens actuated by ferrofluids, Opt. Commun. 284 (8) (2011) 2118–2121.
[20] W. Xiao, S. Hardt, An adaptive liquid microlens driven by a ferrofluidic transducer, J. Micromech. Microeng. 20 (5) (2010) 055032.
[21] L. Dong, H. Jiang, pH-adaptive microlenses using pinned liquid-liquid interfaces actuated by pH-responsive hydrogel, Appl. Phys. Lett. 89 (21) (2006) 211120.
[22] H. Ren, S. Xu, S.-T. Wu, Effects of gravity on the shape of liquid droplets, Opt. Commun. 283 (17) (2010) 3255–3258.
[23] H. Eral, J. Oh, et al., Contact angle hysteresis: a review of fundamentals and applications, Colloid Polym. Sci. 291 (2) (2013) 247–260.
[24] P.-G. De Gennes, F. Brochard-Wyart, D. Quéré, Capillarity and Wetting Phenomena: Drops, Bubbles, Pearls, Waves, Springer Science & Business Media, 2013.
[25] P. Gascoyne, J. Schwartz, J. Vykoukal, F. Becker, Dielectric gate and methods for fluid injection and control, US Patent 6,866,762 (Mar. 15 2005).
[26] P. Liebetraut, P. Waibel, P.H.C. Nguyen, P. Reith, B. Aatz, H. Zappe, Optical properties of liquids for fluidic optics, Appl. Optics 52 (14) (2013) 3203–3215.